Common noncoding *UMOD* variants induce salt-sensitive hypertension and kidney damage by increasing uromodulin expression

Matteo Trudu, Sylvie Janas, Chiara Lanzani, Huguette Debaix, Céline Schaeffer, Masami Ikehata, Lorena Citterio, Sylvie Demaretz, Francesco Trevisani, Giuseppe Ristagno, Bob Glaudemans, Kamel Laghmani, Giacomo Dell'Antonio, the SKIPOGH team, Johannes Loffing, Maria P. Rastaldi, Paolo Manunta, Olivier Devuyst*, Luca Rampoldi*

SUPPLEMENTARY INFORMATION

Supplementary Figures 1–8

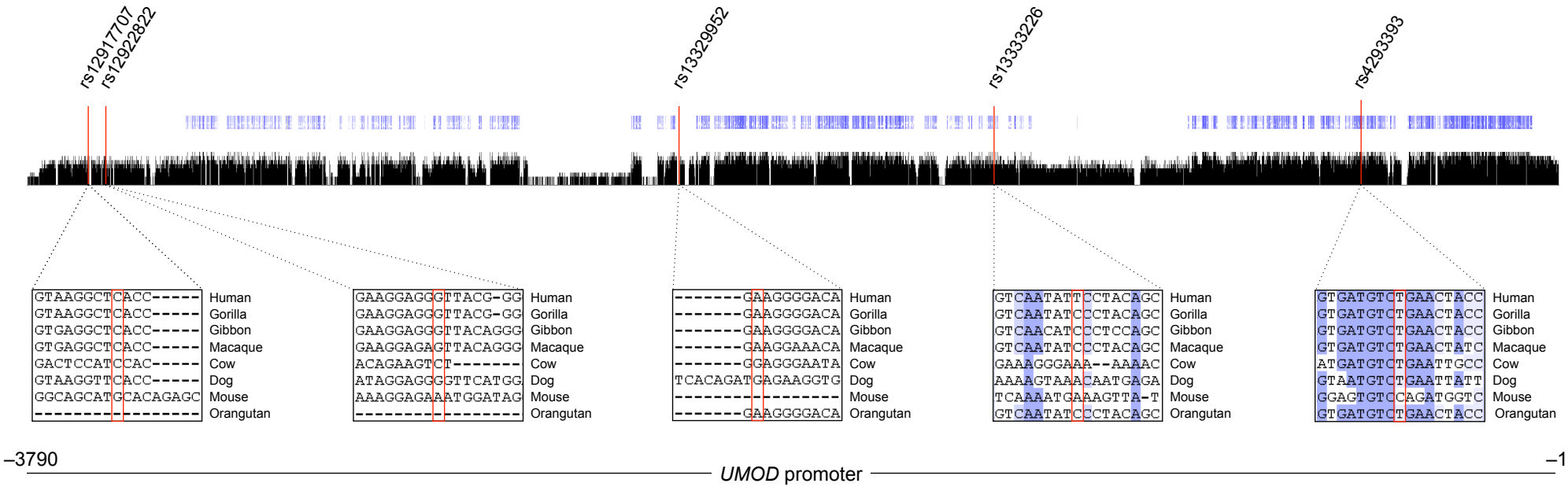

Supplementary Figure 1. Conservation of the *UMOD* promoter sequence. The graphs represent sequence conservation of the 3.79 kb *UMOD* human promoter aligned with gorilla, gibbon, macaque, orangutan, cow, dog and mouse ones. The blue shading is representative of sequence conservation. Black bars represent the percentage of nucleotide identity at each position among the species analyzed. The position of top SNPs that were associated with hypertension and CKD in different GWAS is shown. Each box shows the nucleotide sequence around the SNP (±8 bp).

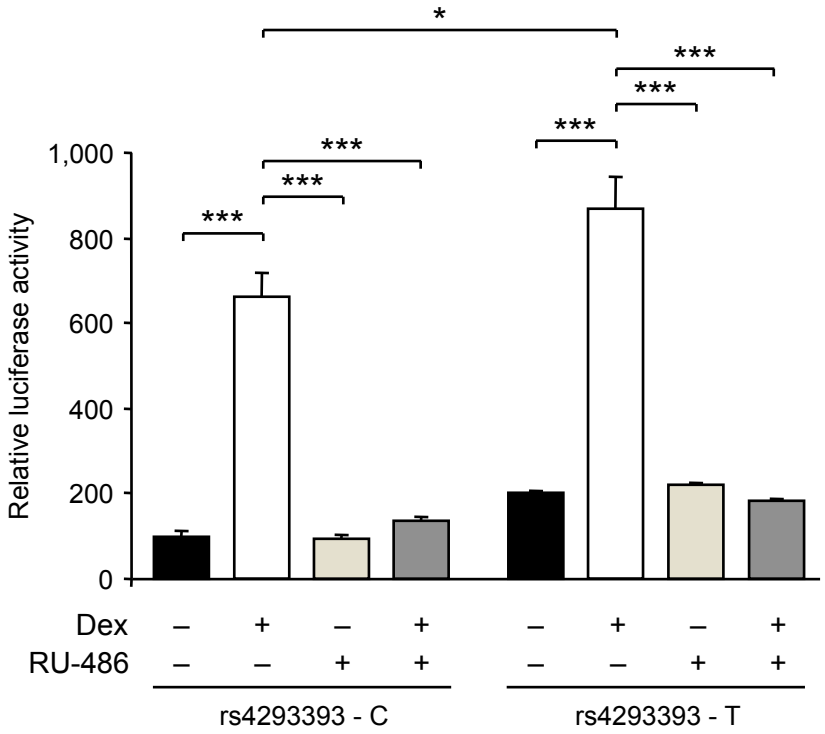

Supplementary Figure 2. Transcriptional activity of the *UMOD* promoter containing protective (C) or risk (T) alleles of SNP rs4293393 in response to glucocorticoids. Luciferase activity was measured after treatment of transfected MKTAL cells with 1 μM dexamethasone (Dex), a potent corticosteroid analog and / or with 10 μM RU-486, a glucocorticoid receptor antagonist. Dexamethasone increases the activity of the *UMOD* promoter. The induction is significantly higher in the presence of the risk allele, while the delta of luciferase activity is slightly higher (+687% vs. +567%), although not significant, in the risk allele. A comparable delta over baseline suggests the presence of additional glucocorticoid response elements in the *UMOD* promoter fragment, as indeed indicated by prediction analysis (data not shown). Dexamethasone induction is fully abolished by treatment with RU-486. Treatment with RU-486 alone has no effect on basal transcriptional activity. The graph is representative of 4 independent experiments. Bars indicate average ± s.e.m. **P* < 0.05; ****P* < 0.001 (ANOVA followed by Bonferroni's test).

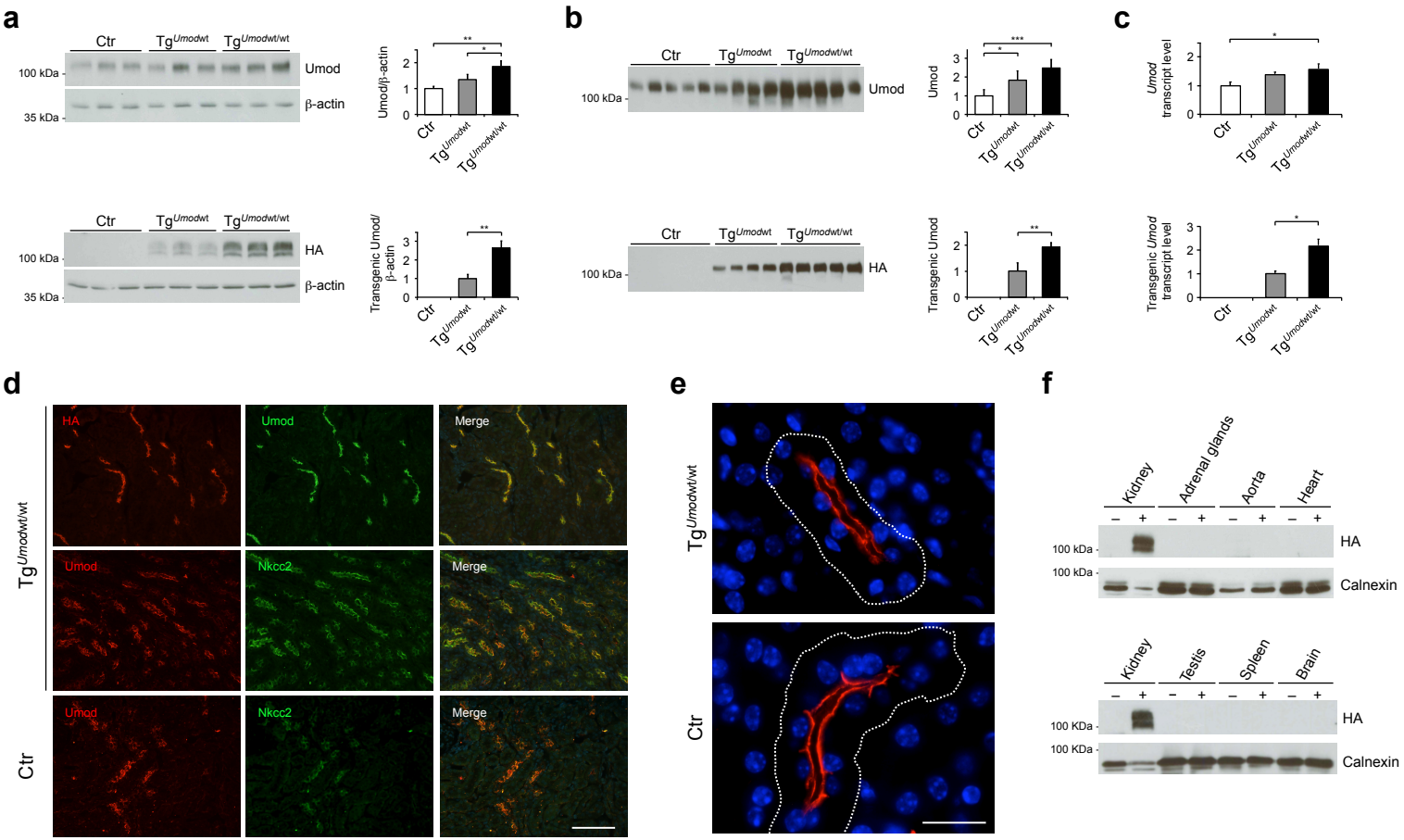

Supplementary Figure 3. Uromodulin expression and localization in *Umod* transgenic mice. (**a**, **b**) Representative immunoblot analyses showing total (Umod) and HA-tagged transgenic uromodulin in kidney lysates (**a**) and urine samples (**b**) from non-transgenic control (Ctr), Tg$^{Umod\text{wt}}$ and Tg$^{Umod\text{wt/wt}}$ mice. Beta actin is shown as a lysate loading control. Urinary protein loading was normalized to urinary creatinine concentration. Relative densitometry of normalized values is shown. (**c**) Relative transcript level of total (upper panel) and transgenic (lower panel) uromodulin in kidneys of control, Tg$^{Umod\text{wt}}$ and Tg$^{Umod\text{wt/wt}}$ mice as assessed by Real-Time qPCR. Overall, protein and transcript expression data show that uromodulin is overexpressed by about 40% and 80% in the kidneys of Tg$^{Umod\text{wt}}$ and Tg$^{Umod\text{wt/wt}}$ mice respectively. Its urinary level is proportionally increased in transgenic mice (n = 5). Each bar represents average ± s.d. (**a**, **b**) or average ± s.e.m. (**c**). *P < 0.05; **P < 0.01; ***P < 0.001 determined by ANOVA followed by Bonferroni's test (**a**, **b**, **c**, upper panels) or unpaired t test (**a**, **b**, **c**, lower panels). (**d**) Immunofluorescence analysis showing total and transgenic (HA) uromodulin co-localization in the kidney of Tg$^{Umod\text{wt/wt}}$ mice (top row). Like in control mice, uromodulin is exclusively expressed in TAL segments in Tg$^{Umod\text{wt/wt}}$ mice, as shown by full co-localization with TAL co-transporter Nkcc2 (middle and bottom rows). Bar = 100 μm. (**e**) Immunofluorescence analysis showing uromodulin distribution in TAL segments of control and Tg$^{Umod\text{wt/wt}}$ mice. In both lines uromodulin is mostly detected on the luminal side of TAL segments demonstrating that uromodulin overexpression does not affect its polarized localization. Bar = 20 μm. Expression data were similar at 6 and 16 months of age. (**f**) Expression of HA-tagged transgenic uromodulin in different tissues lysates from 3 month-old control (–) and Tg$^{Umod\text{wt/wt}}$ mice (+). Transgenic uromodulin is detected in kidney only. Calnexin was used as a loading control.

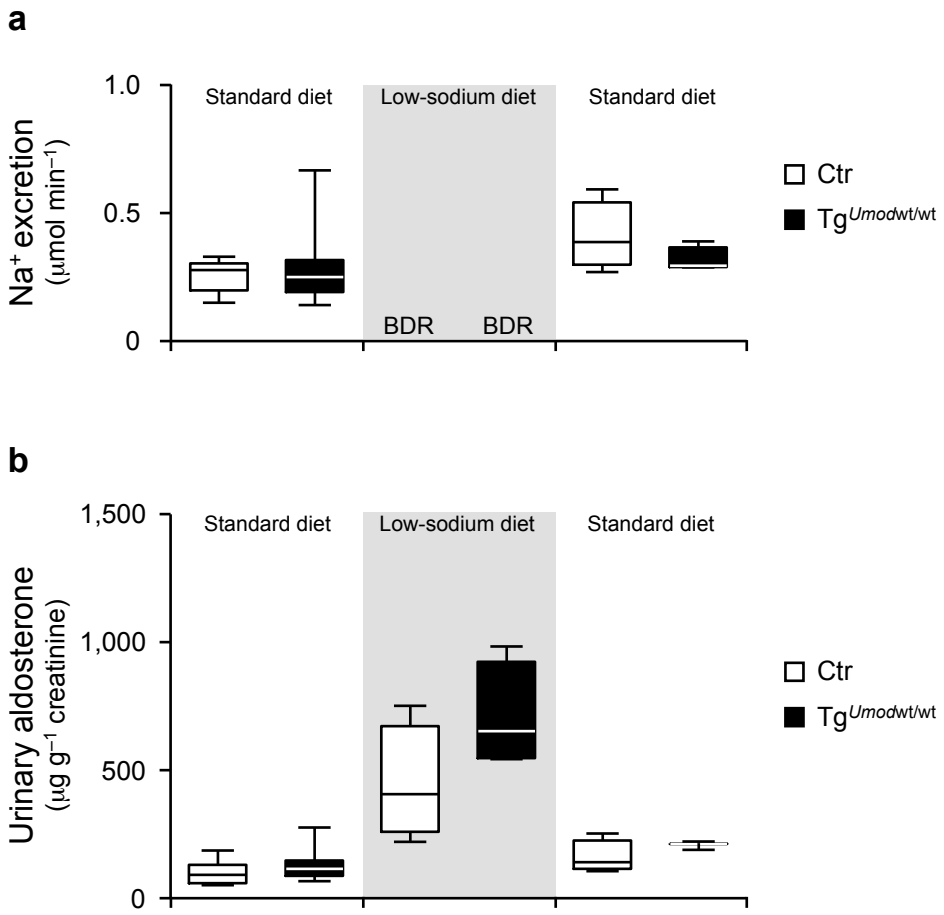

Supplementary Figure 4. Urinary sodium and aldosterone levels in control and Tg$^{Umodwt/wt}$ mice in standard and low-sodium diet. Box and whiskers plot showing Na^+ (**a**) and aldosterone (**b**) in urine of 14 month-old control and transgenic mice fed with standard or low-sodium diet. Urine collections were carried out at baseline, 10 days after start of the low-sodium diet and 10 days after re-establishment of standard diet (standard diet: *n* = 10 per group; low-salt diet: *n* = 4 per group; re-established standard diet: *n* = 4 per group). Bars represent min and max values. No significant difference in sodium balance and aldosterone levels between control and Tg$^{Umodwt/wt}$ mice was observed (Mann Whitney test, two-tailed). BDR, below detection range (<10 mmol L^{-1}).

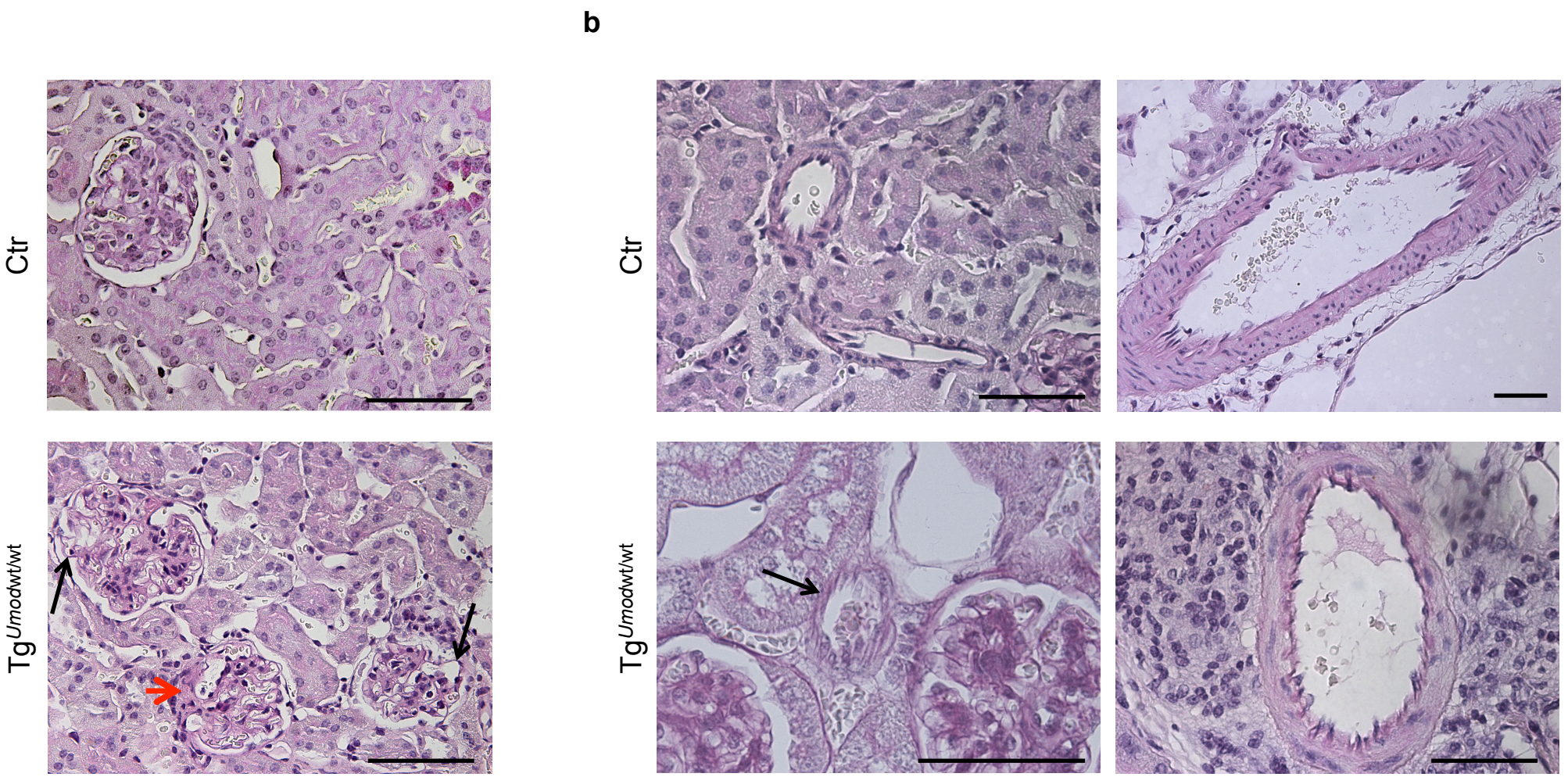

Supplementary Figure 5. Representative renal histological images of 16 month-old control and Tg$^{Umodwt/wt}$ mice. (**a**) The glomerulus and the interstitium of a control mouse show normal features (upper panel). In contrast, glomeruli from a transgenic animal show dilation of the capillary loops (black arrows). Red arrow highlights a segmental sclerotic area in a glomerulus with adhesion of the tuft to the Bowman's capsule. (**b**) Small (left panels) and medium size (right panels) arteries from control and Tg$^{Umodwt/wt}$ mice look completely normal. Quantification of the media thickness confirmed the absence of vascular changes in the kidneys of Tg$^{Umodwt/wt}$ mice (data not shown) (PAS, bar = 100 μm).

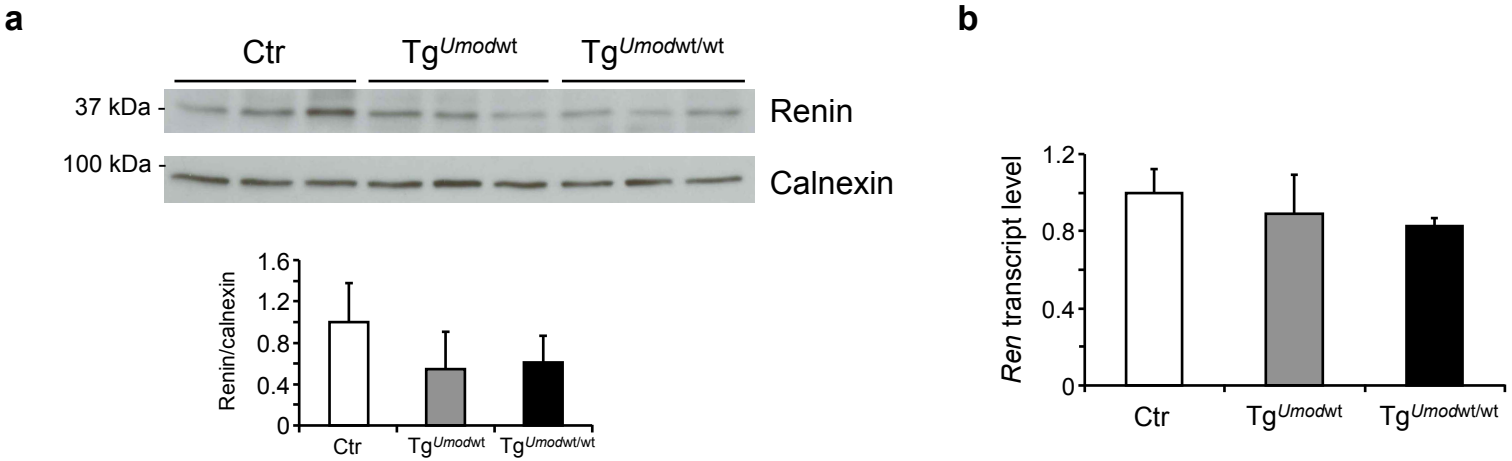

Supplementary Figure 6. Reduced renin expression in *Umod* transgenic mice. (**a**) Representative immunoblot analysis showing renin level in kidney lysates from 16 month-old control, Tg$^{Umod\text{wt}}$ and Tg$^{Umod\text{wt/wt}}$ mice. Calnexin was used as a loading control. Relative densitometric analysis (n = 9 Ctr, 5 Tg$^{Umod\text{wt}}$ and 9 Tg$^{Umod\text{wt/wt}}$) shows a reduction of renin in the kidneys of transgenic mice ($P < 0.05$, ANOVA test). Bars indicate average ± s.d. (**b**) Real-time qPCR on total kidney extracts shows a trend for reduction of relative renin transcript level in transgenic mice (n = 10 Ctr, 5 Tg$^{Umod\text{wt}}$ and 10 Tg$^{Umod\text{wt/wt}}$). Bars indicate average ± s.e.m. (ANOVA followed by Bonferroni's test (**a**, **b**)).

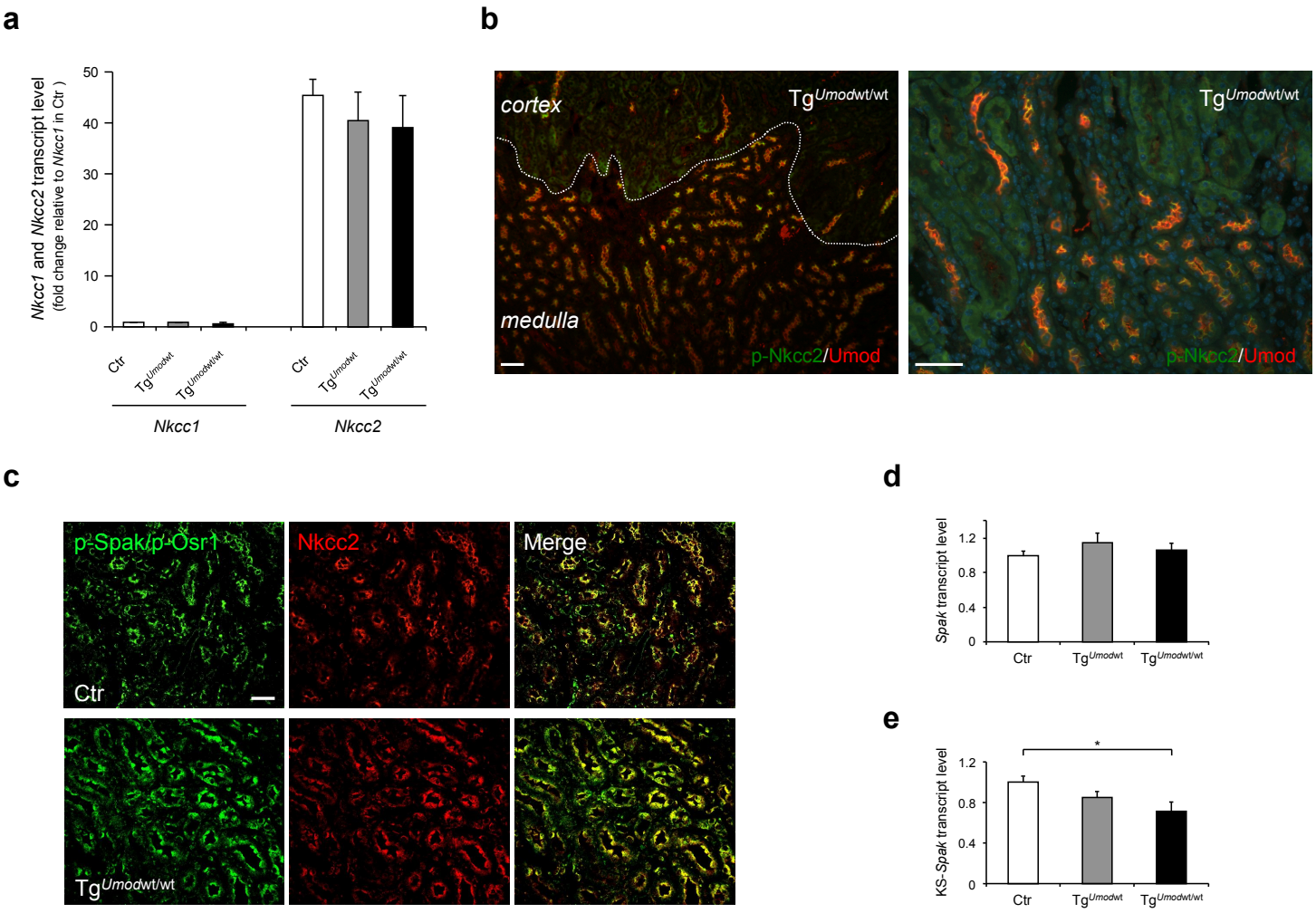

Supplementary Figure 7. Expression of Nkcc1, Nkcc2, Spak and Osr1 in control and *Umod* transgenic mice. (**a**) *Nkcc1* and *Nkcc2* mRNA levels (Real-time RT-qPCR) in kidneys of 16 month-old Ctr, Tg$^{Umod wt}$ and Tg$^{Umod wt/wt}$ (n = 5 per group). In the kidneys of each group, *Nkcc2* expression is about 40 times higher than *Nkcc1*. (**b**) Representative immunofluorescence showing the distribution of p-Nkcc in the kidney of a Tg$^{Umod wt/wt}$ mouse (12 month-old). The vast majority of p-Nkcc corresponds to phospho-Nkcc2, as it is localized at the apical membrane of uromodulin-positive TAL segments. This is consistent with the apical localization of Nkcc2, while Nkcc1 is mainly found at the basolateral membrane of epithelial cells[57]. Bar = 50 μm. (**c**) Immunofluorescence analysis showing phosphorylated Spak/Osr1 (p-Spak/p-Osr1) and Nkcc2 localization in the kidney of 16 month-old control and Tg$^{Umod wt/wt}$ mice. Phosphorylated kinases are mostly enriched in TAL cells, as shown by co-localization with Nkcc2. Bar = 100 μm. (**d**, **e**) Relative transcript levels of full-length *Spak* (**d**) and the splicing isoform KS-*Spak* (**e**), as assessed by Real-Time qPCR on total kidney extracts from 16 month-old control, Tg$^{Umod wt}$ and Tg$^{Umod wt/wt}$ mice (n = 5 per group). Expression of full-length *Spak* is comparable in the three groups analyzed, while the transcript level of KS-*Spak* is reduced in uromodulin transgenic mice. Each bar represents average ± s.e.m. *P < 0.05 (ANOVA followed by Bonferroni's test).

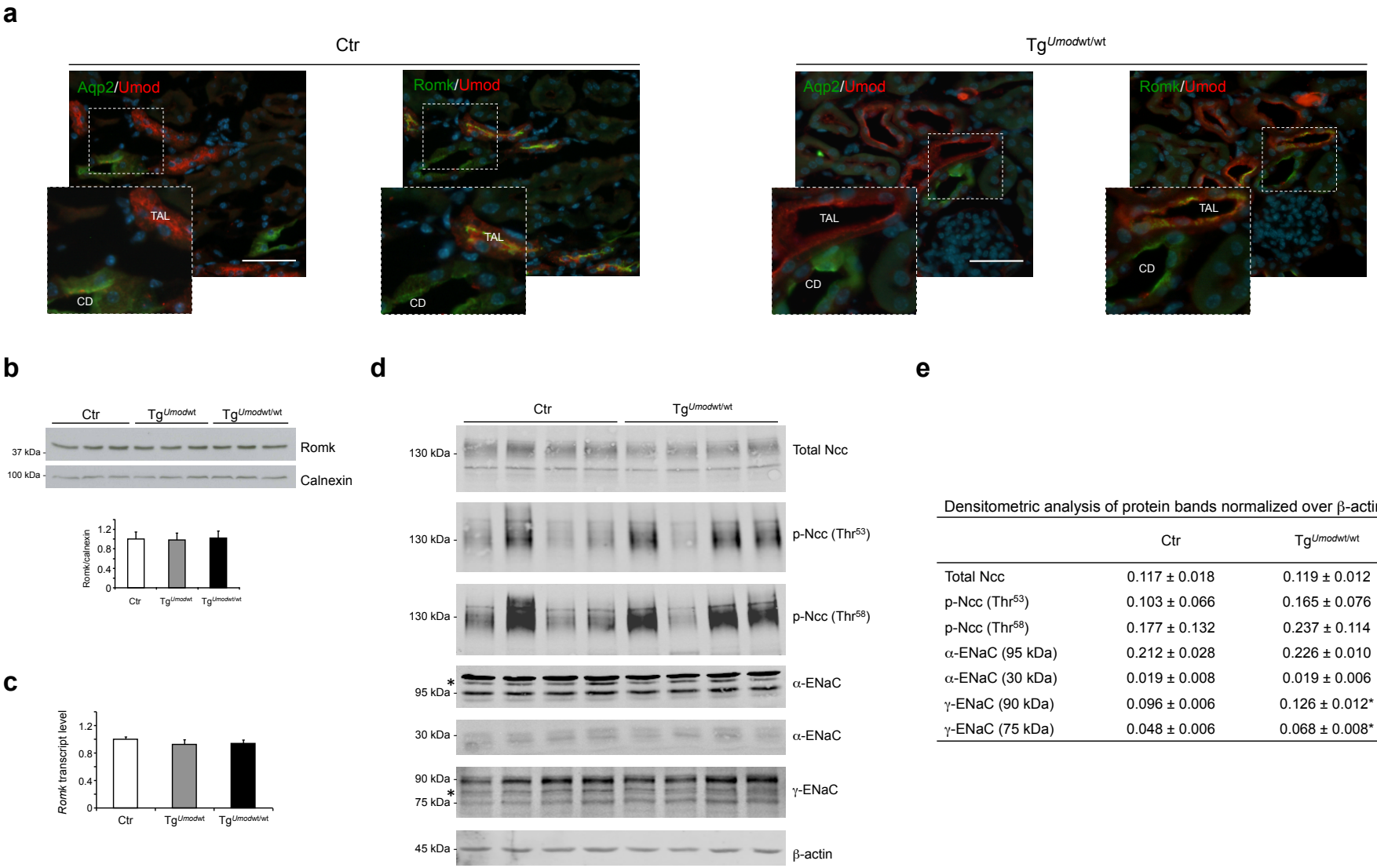

Densitometric analysis of protein bands normalized over β-actin

	Ctr	Tg$^{Umod wt/wt}$
Total Ncc	0.117 ± 0.018	0.119 ± 0.012
p-Ncc (Thr^{53})	0.103 ± 0.066	0.165 ± 0.076
p-Ncc (Thr^{58})	0.177 ± 0.132	0.237 ± 0.114
α-ENaC (95 kDa)	0.212 ± 0.028	0.226 ± 0.010
α-ENaC (30 kDa)	0.019 ± 0.008	0.019 ± 0.006
γ-ENaC (90 kDa)	0.096 ± 0.006	0.126 ± 0.012*
γ-ENaC (75 kDa)	0.048 ± 0.006	0.068 ± 0.008*

Supplementary Figure 8. Romk channel expression and localization and protein levels of Ncc and ENaC sodium transporters in control and Tg$^{Umod wt/wt}$ mice. (**a**) Similar Romk expression and tubular localization in 12 month-old control and Tg$^{Umod wt/wt}$ mice, as assessed in consecutive renal sections (4 μm) co-stained with markers of TAL (uromodulin) or collecting duct (CD) (aquaporin 2, Aqp2) segments. Bar = 50 μm. (**b**, **c**) Romk expression at the protein (**b**) and mRNA (**c**) level (Real-time RT-qPCR) is not different in control and *Umod* transgenic mice (*n* = 5 per group; 16 months of age). Bars represent average ± s.d. in **b** or average ± s.e.m. in **c** (ANOVA followed by Bonferroni's test). (**d**) Immunoblot analysis showing total and phosphorylated (at Thr^{53} or Thr^{58}) Ncc and ENaC alpha and gamma isoforms in kidneys of control and Tg$^{Umod wt/wt}$ (*n* = 4 per group; 16 months of age). Beta actin is shown as a loading control. *unspecific signal. (**e**) Densitometric analysis shows the absence of compensatory downregulation of sodium transporters in distal segments of the nephron in Tg$^{Umod wt/wt}$ mice. *$P < 0.05$ (unpaired *t* test).

Common noncoding *UMOD* variants induce salt-sensitive hypertension and kidney damage by increasing uromodulin expression

Matteo Trudu, Sylvie Janas, Chiara Lanzani, Huguette Debaix, Céline Schaeffer, Masami Ikehata, Lorena Citterio, Sylvie Demaretz, Francesco Trevisani, Giuseppe Ristagno, Bob Glaudemans, Kamel Laghmani, Giacomo Dell'Antonio, the SKIPOGH team, Johannes Loffing, Maria P. Rastaldi, Paolo Manunta, Olivier Devuyst*, Luca Rampoldi*

SUPPLEMENTARY INFORMATION

Supplementary Tables 1–3

Supplementary Table 1. Clinical and biological parameters at baseline in control and Tg$^{Umod wt/wt}$ mice

Measurement	Control	Tg$^{Umod wt/wt}$	*P*
Body weight (BW), g	33.5 ± 2.5	32.3 ± 3.6	NS
GFR (Sinistrin), μL·min^{-1}·100 g BW^{-1}	1735 ± 100	1673 ± 126	NS
Plasma			
Osmolality, mOsm·kg H_2O^{-1}	342 ± 11.5	332 ± 5.8	NS
Creatinine, mg·dL^{-1}	0.12 ± 0.02	0.14 ± 0.05	NS
Urea, mg·dL^{-1}	45 ± 9.5	52 ± 16.7	NS
Uric acid, mg·dL^{-1}	3.5 ± 1.0	2.3 ± 1.3	NS
Na^+, mmol·L^{-1}	152 ± 3.8	149 ± 1.3	NS
K^+, mmol·L^{-1}	7.0 ± 0.8	6.1 ± 1.0	NS
Cl^-, mmol·L^{-1}	113 ± 2.9	111 ± 2.6	NS
Urine			
Creatinine, μmol·g BW^{-1}·14h^{-1}	0.26 ± 0.05	0.27 ± 0.08	NS
Na^+, μmol·min^{-1}	0.25 ± 0.06	0.25 ± 0.07	NS
K^+, μmol·min^{-1}	0.55 ± 0.14	0.50 ± 0.12	NS
Cl^-, μmol·min^{-1}	0.36 ± 0.07	0.32 ± 0.09	NS
Ca^{2+}, μg·min^{-1}	0.06 ± 0.03	0.07 ± 0.03	NS

Data are means ± s.d. *N* = 8 (Ctr) and 6 (Tg$^{Umod wt/wt}$) (12–16 month-old). Urine collections were obtained over 14 h overnight. NS, not significant. Unpaired *t* test.

Supplementary Table 2. Ambulatory blood pressure monitoring and response to furosemide in hypertensive patients carrying protective or risk *UMOD* rs4293393 genotype

ABPM protocol			
Measurement	CC+CT (*n* = 161)	TT (*n* = 310)	*P*
Age, years	44.4 ± 10.1	44.0 ± 8.8	NS
Females (%)	27 (16.8)	53 (17.1)	NS
BMI, $Kg \cdot m^{-2}$	26.0 ± 3.05	25.7 ± 2.82	NS
eGFR, $ml \cdot min^{-1}$	104 ± 9.77	104 ± 8.80	NS
Plasma Renin Activity, $ng \cdot ml^{-1} \cdot h^{-1}$	1.6 ± 1.40	1.6 ± 1.23	NS
SBP, mm Hg	141 ± 0.80	142 ± 0.63	NS
DBP, mm Hg	91 ± 0.66	93 ± 0.50	0.011
Na^+ excretion (24 h), $mmol \cdot L^{-1}$	165 ± 73	167 ± 72	NS
Furosemide test			
Baseline measurement (T0)	CC+CT (*n* = 47)	TT (*n* = 118)	*P*
SBP, mm Hg	146 ± 2.18	148 ± 1.45	NS
DBP, mm Hg	98 ± 1.55	101 ± 0.85	NS
Diuresis, $ml \cdot min^{-1}$ *	1.0 ± 0.4	1.0 ± 0.4	NS
Na excretion, $\mu mol \cdot min^{-1}$ *	111 ± 53	97 ± 39	NS
Furosemide measurement (T240)			*P*
SBP, mmHg	145 ± 2.40	144 ± 1.58	NS
DBP, mmHg	99 ± 1.57	99 ± 0.92	NS
Diuresis, $ml \cdot min^{-1}$ *	6.2 ± 1.9	7.0 ± 1.9	0.013
Na excretion, $\mu mol \cdot min^{-1}$ *	565 ± 140	629 ± 177	0.024
Delta (T240 – T0)			*P*
SBP, mm Hg	-0.9 ± 1.61	-4.3 ± 0.95	(0.060)
DBP, mm Hg	0.47 ± 1.00	-2.0 ± 0.64	0.037
Diuresis, $ml \cdot min^{-1}$ *	5.2 ± 1.9	6.0 ± 1.9	0.045
Na excretion, $\mu mol \cdot min^{-1}$ *	455 ± 164	532 ± 180	0.030

Data are means ± s.d., except for BP measurements that are expressed as means ± s.e.m. The number of patients per group is indicated, except for: * 33 (CC+CT) vs. 94 (TT). One-way ANOVA test. ABPM, ambulatory blood pressure monitoring; SBP, systolic blood pressure; DBP, diastolic blood pressure.

Supplementary Table 3. Allelic and genotypic frequencies of *UMOD* SNP rs4293393 in different populations

Population	Allele T (freq)	Allele C (freq)	Genotype TT (freq)	Genotype TC (freq)	Genotype CC (freq)
MI_HPT	0.820	0.180	310 (0.658)	152 (0.323)	9 (0.019)
SKIPOGH	0.837	0.163	532 (0.696)	214 (0.280)	18 (0.024)
1000GENOMES:ALL	0.832	0.168	759 (0.695)	298 (0.273)	35 (0.032)
1000GENOMES:EUR	0.799	0.201	245 (0.646)	116 (0.306)	18 (0.047)
1000GENOMES:AMR	0.807	0.193	118 (0.652)	56 (0.309)	7 (0.039)
1000GENOMES:ASN	0.927	0.073	246 (0.860)	38 (0.133)	2 (0.007)
1000GENOMES:AFR	0.789	0.211	150 (0.610)	88 (0.358)	8 (0.032)
CSHL-HAPMAP-CEU	0.823	0.177	76 (0.673)	34 (0.301)	3 (0.026)
CSHL-HAPMAP-TSI	0.835	0.165	62 (0.705)	23 (0.261)	3 (0.034)
CSHL-HAPMAP-MEX	0.810	0.190	32 (0.640)	17 (0.340)	1 (0.020)
CSHL-HAPMAP-GIH	0.724	0.276	46 (0.529)	34 (0.391)	7 (0.080)
CSHL-HAPMAP-CHB	0.939	0.061	37 (0.902)	3 (0.073)	1 (0.024)
CSHL-HAPMAP-CHD	0.947	0.053	76 (0.894)	9 (0.106)	0 (0.000)
CSHL-HAPMAP-HCB	0.872	0.128	32 (0.744)	11(0.256)	0 (0.000)
CSHL-HAPMAP-JPT	0.953	0.047	78 (0.907)	8 (0.093)	0 (0.000)
CSHL-HAPMAP-ASW	0.786	0.214	29 (0.592)	19 (0.388)	1 (0.020)
CSHL-HAPMAP-MKK	0.706	0.294	72 (0.503)	58 (0.406)	13 (0.091)
CSHL-HAPMAP-YRI	0.796	0.204	72 (0.637)	36 (0.319)	5 (0.044)
CSHL-HAPMAP-LWK	0.778	0.222	51 (0.567)	38 (0.422)	1 (0.011)

MI_HPT, hypertensive patient cohort[41], and SKIPOGH cohort[42] in the present study. Data from 1000 Genomes (http://browser.1000genomes.org/index.html) and HapMap (http://hapmap.ncbi.nlm.nih.gov/). Alleles refer to the reverse strand genomic sequence. CEU, European ancestry; TSI, Tuscans in Italy; MEX, Mexican ancestry in Los Angeles; GIH, Gujarati Indians in Houston; CHB, Han Chinese in Beijing; CHD, Chinese in Metropolitan Denver; HCB, Han Chinese in Beijing; JPT, Japanese in Tokyo; ASW, African ancestry in Southwest USA; MKK, Maasai in Kinyawa, Kenya; YRI, Yoruba in Ibadan, Nigeria; LWK, Luhya in Webuye, Kenya. Frequencies of the minor allele C in the MI_HPT and SKIPOGH cohorts are similar to the ones observed in reference populations of European ancestry.